

Distribution of heat flux density in spiral heat exchangers

TH. BES and W. ROETZEL

Universität der Bundeswehr Hamburg, Germany

(Received 17 December 1990)

Abstract—An analytical method is developed for the accurate calculation of the temperature changes in countercurrent flow spiral heat exchangers. The spiral is composed of circular arc profiles with the centres of curvature on the angles of an equilateral triangle. Constant overall heat transfer coefficients and heat capacities are assumed. In contrast to the conventional procedure, the heat flux density distribution is considered, which offers considerable advantages over a direct analysis of the fluid temperatures. The influence of various geometrical parameters is investigated and charts are presented for the design and rating of spiral heat exchangers.

1. INTRODUCTION

1.1. Preface

AMONGST the various forms of heat exchangers which are employed in industry for heating or cooling fluids, countercurrent Spiral plate Heat Exchanger (acronym SHE) has found a solid position because of its numerous advantages. High thermal performance, easy maintenance and compactness often prevail over other exchangers. The SHE within such fluids as, for example, untreated water, sludges or slurries, can be met in practice, whereas the other exchangers fail because of hard fouling.

However, despite wide applications, at the present stage of heat transfer theory little is known about ways of finding an exact value of the effectiveness P for SHE, even in its classical use of constant heat transfer coefficients.

In this paper particular stress is laid on the determination of the thermal effectiveness P for SHE with complete accordance in regard to both the physical model of the thermal process as well as to the geometry of an apparatus. This was done in order to take a step towards developing the thermal theory of SHE and especially to study the thermodynamical limitations which a designer meets. A general view of SHE with cross-sections which allow the flow arrangement of fluids to be observed is shown in Fig. 1.

As a by-product this paper could be helpful as a reference in developing approximate methods for calculation of the effectivenesses of SHE.

1.2. Assumptions regarding geometrical and physical models of SHE

The thermal theory of SHE, version Q, is the formal analytical way of dealing with the heat-flux-density vector under conventional assumptions well known in the literature of heat exchangers [1, 2] and taken into account in the analysis of this problem.

In the light of some thermal attributes of SHE such

as:

interesting behaviour in distributions of the heat flux density: possible reversed heat transfer, oscillations;

conditions under which for very high NTU a local maximum for the heat flux density may occur;

and in the light of a simple method of solution, from a mathematical point of view, i.e. the standard technique of Laplace's integral, the Q version offers advantages in comparison to methods which deal directly with temperatures of fluids. Furthermore, it is possible to express the formula for a calculation of the effectiveness of SHE explicitly.

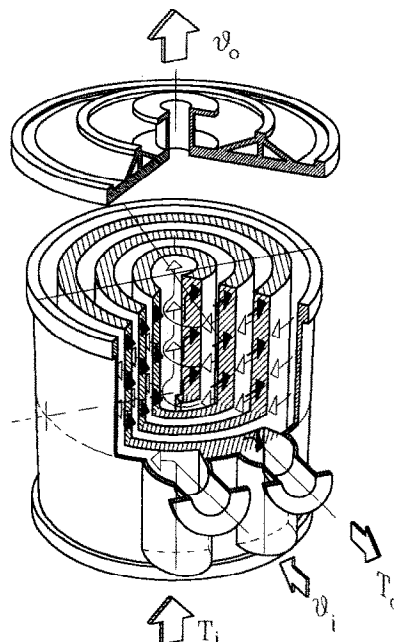


FIG. 1. Cross-sections of counterflow spiral plate heat exchanger.

NOMENCLATURE

A_0	total surface area [m ²]	TCHE	acronym, True Countercurrent Heat Exchanger.
b	channel spacing which was optionally chosen as a unit of length [m]	Greek symbols	
C	heat capacity rate [W K ⁻¹]	Δ_l	local temperature difference along main spiral, $T_l - \vartheta_{l+1}$
F	log mean temperature difference correction factor	Δ_{l+1}	local temperature difference along side spiral, $T_{l+2} - \vartheta_{l+1}$
h_0	height of exchanger [m]	ϑ	dimensionless temperature, t_{II} , real temperature of fluid II, $(t_{II} - t_{II,o}) / (t_{I,i} - t_{II,o})$ [K]
k	overall heat transfer coefficient [W m ⁻² K ⁻¹]	ϕ	total angle measured from beginning of the spiral, $2\pi l + \varphi$ [rad]
M	matrices (see equations (7) and (8))	φ	angle in coordinate system (r, φ) , Fig. 3 [rad]
n	number of channels in SHE equal to double number of turns	ψ	cross-sectional number of transfer units, $2\pi k h_0 b / C_1$
NTU	number of transfer units, $A_0 k / C$	ω	auxiliary variable, $\varphi \psi$.
P	effectiveness of SHE	Subscripts	
q_l, q_{l+1}	reduced heat flux density defined differently for even and odd numbers l in equation (5)	i	inlet
R	heat capacity rate ratio for counter flow, C_{II} / C_I	o	outlet
r	radius measured in b units	I	fluid I
s	Laplace's parameter	II	fluid II
SHE	acronym, countercurrent Spiral plate Heat Exchanger	$j, A; j, B; j, C$	channel j in sector A, B, C.
T	dimensionless temperature, t_I , real temperature of fluid I, $(t_I - t_{II,o}) / (t_{I,i} - t_{II,o})$ [K]		

The above assumptions include the geometry of the apparatus and also the properties of fluids. The assumption related to the geometry of SHE follows the model of a spiral described in ref. [3] which is an involute of a polygon. However, in the calculations done in the present paper the equilateral polygon (triangle: see Fig. 2) was chosen as a basis for SHE, as distinct from the segment of a line which, as a degenerate form of polygon, was considered in ref. [3].

It was proven on the basis of numerical data that the present assumption about a spiral built on the basis of a triangle instead of the segment of a line exceeds superfluously demands of accuracy even for the purpose of getting a proper level of reference. This was done in order to approach the actual model of involute to the model of Archimedes' spiral, which is almost overwhelmingly considered in the literature on SHE [4-8].

The main assumptions about fluids' properties and flow conditions agree with the assumptions known from the theory of heat exchangers [1, 2], which from now on will be called 'standard assumptions'. These are:

- heat is transferred only by convection;
- no change of phase, steady flow of fluids and heat;
- temperatures are equalized across a channel;

- constant overall heat transfer coefficient;
- constant heat capacities of fluids and no heat losses to the environment;
- heat conduction throughout the walls occurs only in the direction perpendicular to the surface.

A very common arrangement of flows in this type of exchanger is spiral flow in both channels. The fluids usually flow countercurrently, with the cold fluid entering at the periphery and flowing in towards the centre, and the hot fluid entering at the centre and flowing towards the periphery (hot and cold fluid could also be exchanged). The arrangement of flows is shown in Fig. 2.

All quantities considered in this paper are expressed in dimensionless form.

2. SURVEY OF LITERATURE

Of many publications dealing with SHE those chosen consisted of either a significant contribution to the thermal theory of countercurrent SHE or used numerical methods of calculation, accomplishing thoroughly the assumptions of the physical model of the apparatus.

Reference [9] from 1959/60 is one of the first papers where the properties of SHE were rendered in an analytical way. Instead of an analysis of fluids flow in

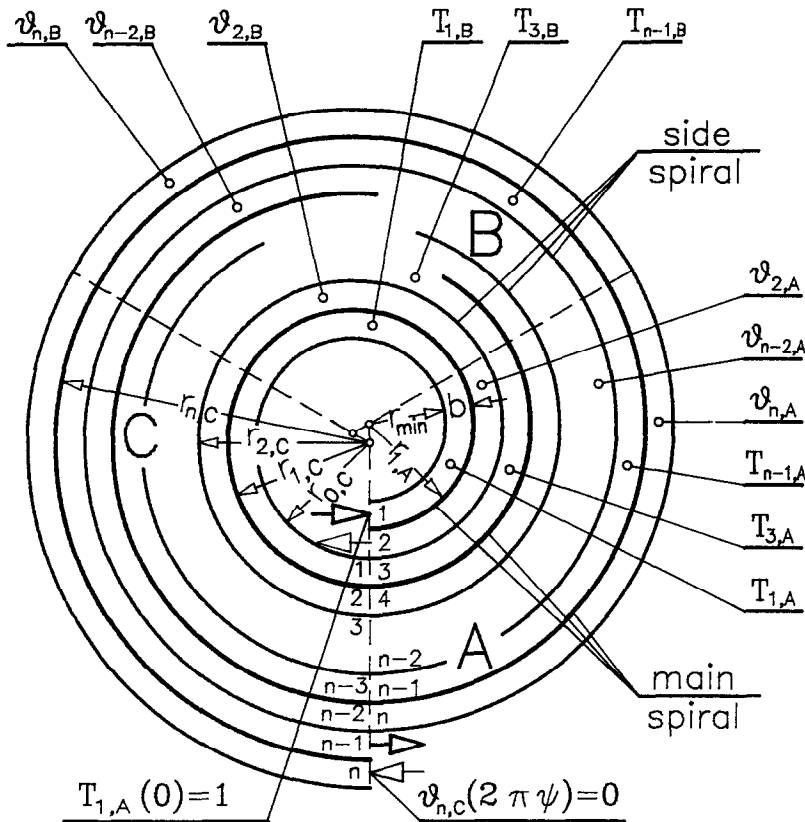


FIG. 2. Arrangement of flows in spiral heat exchanger.

spiral channels, Woschni [9] considered an equivalent plate heat exchanger. The analysis was limited to only a few turns: $2\frac{1}{2}$ checking both channels with hot and cool fluids together.

Later, two papers [4, 6]† appeared in the literature on SHE where thermal analysis including the appropriate assumptions were done correctly in the manner formulated in the standard literature on heat exchangers. Madejski [4] and Zaleski and Krajewski [6] initiated a new idea of solving the problem of SHE in thermal aspect; however, the necessary simplifications proposed there were very poorly controlled from a mathematical point of view, which badly affects the accuracy of the numerical results.

In ref. [10] in 1969, adopting linear and/or parabolic interpolations, Nowak solved the problem without simplifications using the numerical technique of calculation. Later, in 1972, he used a different method of solving this problem which allows one to transfer it to a Cauchy-type problem.

Another numerical attempt towards a solution of the problem is presented in Buonopane and Troupe [5]. To support their experimental data the authors have calculated effectivenesses of SHE using the

Runge-Kutta‡ method to integrate the set of differential equations which represent the energy balances.

The first analytical attempt towards an accurate determination of the effectiveness of SHE regarding the standard assumptions of the literature is presented by Cieslinski and Bes [7]. As a geometrical basis of SHE, the spiral of Archimedes has been chosen. To fulfil the last assumption, well accepted in the literature, the method of orthogonal Hermite polynomials was selected. Despite accordance to the physical and geometrical models and to the standard assumptions due to its complexity, the method cannot be easily accepted by a designer, which reduces its applicable value.

Martin *et al.* [11] proposed the new straightforward formula for the F correction factor of SHE. Because this formula was an approximate approach it needed to be verified with the exact data. This necessary set of data was calculated using the Runge-Kutta method of integration of energy balance equations.

† The authors did not succeed in identifying the original paper where this idea of a solution to the problem was taken from.

‡ In mathematical literature this method is known to be fast and is one of the most effective, but it demands a knowledge of the initial vector of the sought function. In the case of SHEs direct fulfilment of this condition is impossible because the initial n -dimensional vector of temperature has to be found iteratively. That makes the applicability of this method to SHE with a higher number of turns extremely difficult.

In 1984, the first author of this paper proposed a new construction of the spiral as the geometrical basis of SHE [3]. Instead of an Archimedes' spiral which hitherto was commonly found in the literature the new spiral was traced as an involute of a regular polygon. As a consequence, energy balance equations were expressed by a set of ordinary differential equations with constant coefficients. The sought after temperatures of fluids were found by using Laplace's technique of transformation.

In ref. [8] a particular stress is laid on the influence of geometric structures, such as angles of an entrance to and exit from SHE, dimensions of channels, heat transfer area and number of turns, on the basis of heat transfer characteristics. Regarding the numerical evaluations of their proposals Morimoto and Hotta [8] have chosen the aforementioned Runge-Kutta method of integration.

The computational method of thermal design of SHE is the subject of ref. [12]. As the basis of the spiral, Zhang *et al.* proposed the set of semicircles which is the same geometrical construction suggested in ref. [3], namely an involute from a segment of a line. However, regarding a solution of the energy balance equations the approximation proposed in ref. [12] is based on the replacement: derivatives of enthalpy by their difference. Those changes were done regarding the too long way of integration, which is arbitrarily chosen and equal to one half of a turn. This causes poor accuracy of numerical results especially for high values of *NTU*.

3. ANALYTICAL TREATMENT

3.1. Energy balance for spiral heat exchanger

In order to solve the problem analytically, equations should be derived to represent mathematically the energy balance for each of both fluids as well as for each 'turn' of SHE.

All subsequent reasoning in this section can be simplified if the cross-section of the SHE is divided into sectors. This is a consequence of the chosen method of construction of the spiral. Since this spiral is an involute from an equilateral triangle (see Fig. 2) then an area of the SHE has three sectors which are denoted with subscripts A, B and C. The notation of the energy balance in each of these sectors has the same structure and thus it is enough to write this balance for only one sector. Different heat transfer conditions in SHE suggest a conventional subdivision of the single sector into three regions: central with the innermost 'turn', main region with proper 'turns' and rand region with one outermost 'turn'.

Consider the elementary wedge which was cut out from the exchanger along its axis. In Fig. 3 arrows and accompanying formulas symbolize changes in enthalpy of fluids and heat flux densities which occur on the way of arc (*r dφ*).

For the fluid being cooled and flowing in the innermost 'turn', a differential equation with unknown

temperatures *T*₁ and *θ*₂ is given by:

$$-\frac{dT_1}{d\omega} = r_1(T_1 - \theta_2). \tag{1}$$

As an independent variable the product of the constant parameter *ψ* and angle *φ* was chosen: *ω* = *ψφ*. The main region of the analysed section embraces 'turns' where the fluids are heated or cooled throughout both bordered walls. Then for the 'turn' next to innermost as well as other 'turns' the energy balance is represented by differential equations

$$-R \frac{d\theta_j}{d\omega} = r_{j-1}(T_{j-1} - \theta_j) + r_j(T_{j+1} - \theta_j) \tag{2}$$

$$-\frac{dT_{j+1}}{d\omega} = r_j(T_{j+1} - \theta_j) + r_{j+1}(T_{j+1} - \theta_{j+2}) \tag{3}$$

where subscript *j* = 2, 3, 4, . . . , *n* - 2.

Since the fluid in the outermost turn is only heated from one side the differential energy balance for it consists of one term of heat flux on the right hand side of the equation

$$-R \frac{d\theta_n}{d\omega} = r_{n-1}(T_{n-1} - \theta_n). \tag{4}$$

The system of equations (1)–(4) has to be supplemented by boundary conditions which are discussed in Section 3.3.

3.2. Essential principles of Q notation

The objective of further considerations is to employ such a notation which allows us to achieve considerable advantages by solving the problem from both an engineering and mathematical point of view.

Let us assume that the heat transfer through the wall may be represented by dimensionless expressions:

$$\left. \begin{aligned} q_l &= \sqrt{(r_l)}(T_l - \theta_{l+1}) \\ \text{and} \\ q_{l+1} &= \sqrt{(r_{l+1})}(T_{l+2} - \theta_{l+1}). \end{aligned} \right\} \tag{5}$$

Subscript *l* is equal to odd numbers 1, 3, 5, . . . , *n* - 5, *n* - 3, *n* - 1. With uniform numeration *j* = 1, 2, 3, 4, . . . , *n* - 3, *n* - 2, *n* - 1 the values *q_j* could be considered as components of the vector in which elements *q_j* with odd number *j* are proportional to the heat flux density passing throughout the main spiral and with even number *j* to the heat flux density passing the side spiral wall (see Fig. 2). Further, *q* is called the heat flux density, although it deviates from the usual definition.†

If the components of vector *q* are denoted by definition (5) then the conversion of the energy balance equations (1)–(4) may be done by the following procedure: first let one calculate derivatives of *q* with respect to *ω* and next set the formulas (1)–(4) instead of the derivative of temperatures.

As a result, the thermal behaviour of SHE can be

† The definition (5) is convenient for the further technique of mathematical solution.

and homogeneous as well. Additionally, in this way the unsymmetrical matrix of set (1)–(4) was converted into the symmetrical matrix (7) which has considerable advantages for the search of eigenvalues (roots) of this matrix.

3.3. Boundary conditions

Any sector has one set of equations (6) with $n - 1$ derivatives of the heat flux densities which can be solved in any mathematical way. Any solution introduces $n - 1$ constants which have to be determined.

The boundary conditions for vector \bar{q} are formulated upon a principle that assumes the continuity of temperatures in the exchanger and upon the data of given inlet and outlet temperatures.

Let us consider the three sectors A, B and C shown in Fig. 2. The notation of boundary conditions on passages from one sector to another without inlet and outlet of fluids, that is from A to B and B to C, is simple because it follows the principle of temperature continuity:

$$\frac{q_{j,A}(2\pi\psi/3)}{\sqrt{r_{j,A}}} = \frac{q_{j,B}(2\pi\psi/3)}{\sqrt{r_{j,B}}}$$

and

$$\frac{q_{j,B}(4\pi\psi/3)}{\sqrt{r_{j,B}}} = \frac{q_{j,C}(4\pi\psi/3)}{\sqrt{r_{j,C}}} \tag{9}$$

where subscript j runs through all values 1, 2, ..., to $n - 1$. Passing from the first to the last sector where inlet and outlet of fluids take place, i.e. A to C, one can write the conditions in a similar way as before

$$\frac{q_{j+1,A}(0)}{\sqrt{r_{j+1,A}}} = \frac{q_{j-1,C}(2\pi\psi)}{\sqrt{r_{j-1,C}}} \tag{10}$$

but this statement is valid only for $j = 2, 3, 4, \dots, n - 2$. This means that relation (10) gives only $n - 3$ boundary conditions. Two missing conditions should be deduced from given temperatures at the inlet and outlet: $T_{1,A}(0) = 1$ and $\vartheta_{n,C}(2\pi\psi) = 0$ (see Fig. 2).

Consider the situation where the starting vector $\bar{q}_A(0)$ with $n - 1$ functions is known, i.e. with accuracy up to constants of integration, and a general solution of equations (6) for all sectors was found. This allows one to integrate equation (1) since functions on the right hand side of this equation $r_i (T_i - \vartheta_i) = \sqrt{r_i} q_i(\omega)$ are known.

First, remembering that $T_{1,A}(0) = 1$, second using definition (5)

$$q_{1,A}(0) = \sqrt{r_{1,A}}[1 - \vartheta_{2,A}(0)];$$

$$q_{2,A}(0) = \sqrt{r_{2,A}}[T_{3,A}(0) - \vartheta_{2,A}(0)]$$

and third applying equality $T_{1,C}(2\pi\psi) = T_{3,A}(0)$ (Fig. 2), one can write:

$$1 - T_{1,C}(2\pi\psi) = \frac{q_{1,A}(0)}{\sqrt{r_{1,A}}} - \frac{q_{2,A}(0)}{\sqrt{r_{2,A}}}$$

and

$$\frac{q_{1,A}(0)}{\sqrt{r_{1,A}}} - \frac{q_{2,A}(0)}{\sqrt{r_{2,A}}} = \int_{(\Lambda,B,C)} \sqrt{r_1} q_1(\omega) d\omega \tag{11}$$

where integration goes throughout all sectors: A, B and C. The function $\sqrt{r_1} q_1(\omega)$ under an integration sign means $\sqrt{r_{1,A}} q_{1,A}$, $\sqrt{r_{1,B}} q_{1,B}$, $\sqrt{r_{1,C}} q_{1,C}$, respectively when passing through sectors A, B and C. Equation (11) is the first missing condition.†

The second missing relation results from a notation of all components $q_{j,A}$, $q_{j+1,A}$ of the vector \bar{q} on the border line between the sectors A and C. In accordance with definition (5) all temperatures which appear there have to be eliminated.

Thus $\sum (-1)^j q_{j,A}(0)/\sqrt{r_{j,A}}$ is equal to $1 - \vartheta_{n,A}(0)$ where subscript j in the sum runs from $j = 1$ to $j = n - 1$. Dimensionless temperature $\vartheta_{n,A}(0) = \vartheta_{n-2,C}(2\pi\psi)$ can be expressed with the help of components $q_{n-1,C}(2\pi\psi)$, $q_{n-2,C}(2\pi\psi)$ and condition $\vartheta_{n,C} = 0$. As a consequence a formula appears

$$\frac{q_{n-1,C}(2\pi\psi)}{\sqrt{r_{n-1,C}}} - \frac{q_{n-2,C}(2\pi\psi)}{\sqrt{r_{n-2,C}}} + \sum_{l=1}^{j=n-1} (-1)^l \frac{q_{l,A}(0)}{\sqrt{r_{l,A}}} = 1. \tag{12}$$

As a whole the relations (9)–(12) create the set of boundary conditions which allows one to solve this problem completely in explicit form.

3.4. Forms for heat fluxes in SHE

Suppose now that all eigenvalues s_l , $l = 1, 2, 3, \dots, n - 2, n - 1$, of the matrix (7) were found. Due to the Q notation it is easy to check that the matrix (7) is symmetric and therefore all s_l are real and different [13].

For the set of initial values of heat flux density $q_{j,A}(0)$ (temporarily unknown), Laplace's method of transformations gives a general solution satisfying the set (6). In each sector with subscripts $m := A, B$ or C this solution takes the form

$$q_{j,m}(\omega) = \sum_{l=1}^{n-1} q_{l,m}(0) \sum_{l=1}^{n-1} c_{jl} e^{s_l \omega} \tag{13}$$

where c_{jl} is the single residue calculated from the

† It is worthwhile mentioning that the number of mathematical operations can be reduced by only solving the system (9), (10) and (11) having a range equal to $n - 2$, that is one less than before. This is so because these equations have no free terms and as a consequence they can be divided by only one of the unknown values $q_{j,A}(0)$, e.g. $q_{1,A}(0)$, and then solved with respect to quotients: $q_{j,A}(0)/q_{1,A}(0)$ for $j = 2, 3, \dots, n - 2, n - 1$. To determine the last value, $q_{1,A}(0)$, equation (12) is appropriate.

following formula :

$$c_{ji} = \operatorname{res}_{s=s_i} \frac{N_{ij}(s)}{M(s)} = \lim_{s \rightarrow s_i} (s-s_i) \frac{N_{ij}(s)}{M(s)} = \frac{N_{ij}(s_i)}{\left. \frac{dM(s)}{ds} \right|_{s=s_i}} \quad (14)$$

The numerator $N_{ij}(s)$ denotes the matrix $|sI + M(s)|$ in which elements of rows numbered as j and columns numbered as i were replaced in this manner so that they are now equal to 0, with the exception of one which lies at the crossing i and j , and which is equal to 1.

Now, consider the set of unknown values $q_{j,\Lambda}(0)$ ($j = 1, 2, 3, \dots, n-2, n-1$) which has to be found. On the basis of boundary conditions (9), the set of fluxes $q_{j,B}(2\pi\psi/3)$ and $q_{j,C}(4\pi\psi/3)$ could be expressed by the set of values $q_{j,\Lambda}(0)$.

Finally, the unequivocal determination of the sought after values $q_{j,\Lambda}(0)$ is possible from equations (9)–(12), which as a whole makes the system of the equations of $n-1$ range that is equal to the number of unknown components $q_{j,\Lambda}(0)$.

All the above mentioned equations are linear and algebraic and that fact allows one to express all of the components for vector q_A , q_B and q_C explicitly. This statement is valid for the one particular component $q_{n-1,C}(2\pi\psi)$ as well. Thus, the sought form of the effectiveness P_1 can be presented as follows :

$$P_1 = NTU_1 \vartheta_{n-1,C}(2\pi\psi) = NTU_1 q_{n-1,C}(2\pi\psi) / \sqrt{(r_{n-1,C})} \quad (15)$$

The formula (13), together with equation (5), allow one to calculate the temperatures for both fluids at any coordinate on the main or side spiral. Therefore the task of formulating the thermal theory in the Q-version for SHE is complete.

4. LOCAL TEMPERATURE DIFFERENCE IN SHE

Consider the temperature differences between fluids flowing along the walls, which are traced by the main and side spirals. Denote this difference analogous to the definition in equation (5) :

$$\Delta_l(\omega) = T_l(\omega) - \vartheta_{l+1}(\omega)$$

and

$$\Delta_{l+1}(\omega) = T_{l+2}(\omega) - \vartheta_{l+1}(\omega) \quad (16)$$

where subscript l takes odd numbers 1, 3, 5, ..., $n-3$, $n-1$ as before. For example, let us show the run of temperature difference vs total angle as coordinates. Assume as constant : ratio $R = 1$, number of channels $n = 10$ and radius $r_{\min} = 5$, but consider different values of $NTU = 1, 2, 3, 4, 5, 6, 8, 10, 15, 20, 25, 30, 35, 40$ and $NTU = 11.267$. For the last value, effectiveness P_1 approaches its maximum. Results of calculations are shown in Fig. 4.

4.1. Difference of temperatures for main spiral (Fig. 4(a))

It is worth mentioning that for sufficiently high values of NTU the temperature difference Δ_l between fluids separated by the wall placed along the main spiral starts to oscillate with cycle 2π and these oscillations increase with further growth of NTU . This result occurs due to the influence of the different inside and outside heat transfer conditions in the inner- and outermost turns of SHE. The effect of outermost turns is much stronger than of innermost because a wall for the outermost turn is longer than for the innermost. Therefore the larger the value NTU the greater the influence of the outermost turn on the temperature distributions in SHE. This fact cannot be neglected in a thermal analysis.

Another property of the Δ_l function is its maximum, which occurs between the inlet and outlet of fluids and for, e.g. $R = 1$, shifts from outside towards the centre of apparatus together with an increase of NTU . However, this maximum diminishes and then disappears with an increase of the rate ratio R over 1 or a decrease below 1.

4.2. Difference of temperatures for side spiral (Fig. 4(b))

At the start for small, middle or even high values of NTU the difference Δ_{l+1} decreases monotonously. However, it has to be noted that beginning from a certain value of NTU the difference Δ_{l+1} becomes negative. This means that energy transferred from a hotter fluid to a cooler one in a region close to the innermost turn is returned in the main region of the exchanger to that fluid which primarily had the task of heating the cooler one. This contradicts the main function of any heat exchanger. Therefore this negative feature should be an indication and warning to a designer that SHE meets its thermal limits with growth of NTU . However, these values of NTU are very high and rarely occur in practice. Further increase of NTU causes oscillations of Δ_{l+1} similar to that which appears for Δ_l .

5. THERMAL PERFORMANCE OF SPIRAL HEAT EXCHANGER

5.1. Influence of minimal radius of SHE on its effectiveness

As stated in refs. [3, 7], the influence of minimal radius on the thermal effectiveness is very small. It is probably for this reason that in the other papers [5, 11, 12] which deal with thermal calculations of SHE the question of r_{\min} was passed over without comment. However, this problem cannot be ignored when the exact calculation of SHE comes under consideration, either as a contribution to the theory of SHE or as a reference level for approximate methods. Then the dependence P on r_{\min} has to be estimated qualitatively

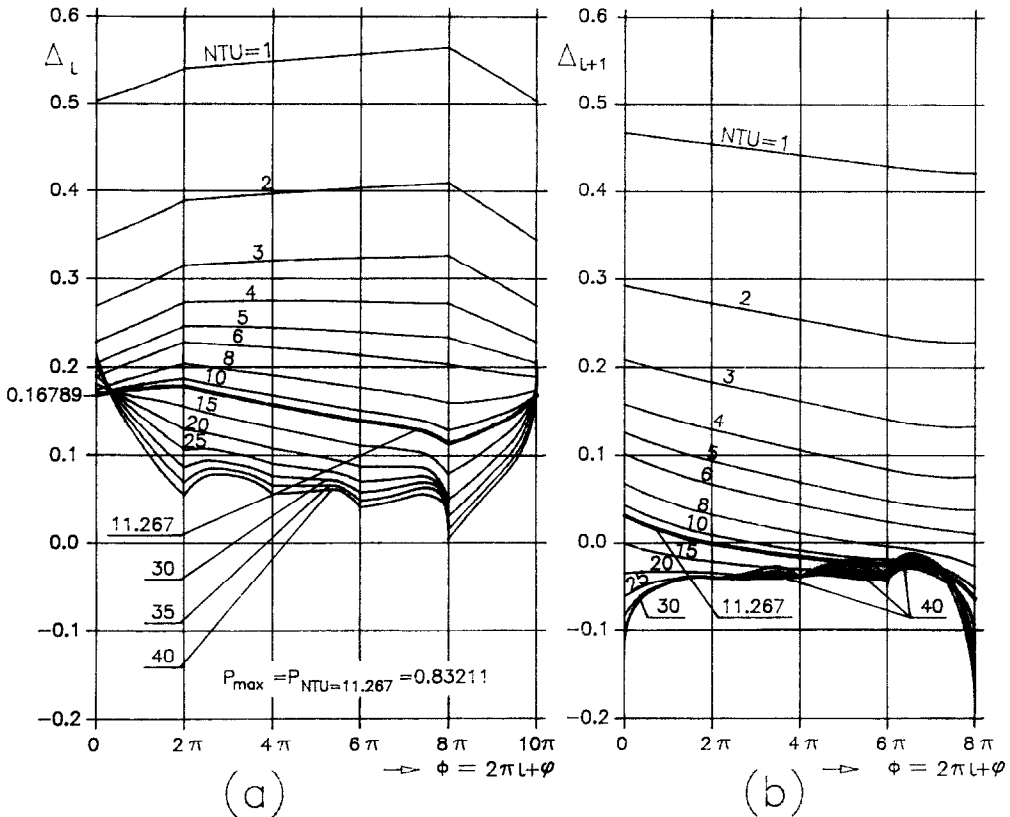


FIG. 4. Local temperature difference Δ vs total angle in SHE. (a) Δ_L along the main spiral. (b) Δ_{L+1} along side spiral for ratio $R = 1$, $n = 10$ channels (five turns) and $r_{min} = 5$. For $NTU = 11.267$, difference $\Delta_L = 0.16789$ achieves a minimum.

and quantitatively, at least in the cases of those parameters where this influence is the greatest.

In practice one can meet the SHE with minimal radii r_{min} from 1 to 30–40 measured in the distance of channels b . The biggest deviations of effectiveness calculated using different r_{min} are expected for ratio $R = 1$ and high values of NTU .

Since the mentioned absolute differences are of the order of 1% it will be convenient to use the excess of default effectiveness over the value of effectiveness calculated for $r_{min} = 0$: this can be denoted

$$\Delta P_r = P(NTU, R, n, r_{min}) - P(NTU, R, n, 0). \quad (17)$$

The parameter NTU has a significant contribution to the value ΔP_r . For a practical interval of NTU values, i.e. 5, and even up to 15 or 20, an increase in NTU causes a slight rise of the effectiveness at constant radius r_{min} . If r_{min} grows further, e.g. to 60, 80 or 100, then the difference ΔP_r changes its sign and rapidly becomes negative.

For ratio $R = 1$, for number of channels $n = 10$, 20, 30 and 40, and for quantities of minimal radius $r_{min} = 1, 2, 5, 10, 20$ and 50, the change of ΔP_r vs $1/NTU$ is shown in Fig. 5.

The curves with higher quantities r_{min} , e.g. 20 or 50,

are shown in Fig. 5, not because of their practical application in cases of small numbers of turns $n = 10, 20, 30$ or 40, but to demonstrate a behaviour of SHE and to prove that further growth of r_{min} does not affect the effectiveness of an exchanger, which for $r_{min} \rightarrow \infty$ achieves an asymptotic value.

Consider again the most practical domain of $NTU < 5$ and cases with small number of turns $n = 10$ and 20 where r_{min} is equal to or smaller than 5 and 10. Then from Figs. 5(a) and (b) it can be seen that deviations of effectiveness ΔP_r due to r_{min} are smaller than 0.8% or 0.4%, respectively. Furthermore, on the basis of Figs. 5(c) and (d) one can anticipate that the higher number of turns, the smaller is the deviation ΔP_r which does not exceed 0.2%.

5.2. Diagrams with effectivenesses P_1 and P_{11} on both axes

To illustrate the theory under discussion, a considerable set of numerical data was computed for a countercurrent flow exchanger. However, nothing stands in the way of extending the calculations to cocurrent flow. This was omitted here because of the small practical use of this kind of exchanger.

Amongst the many ways which allow a demonstration of the thermal properties of any heat ex-

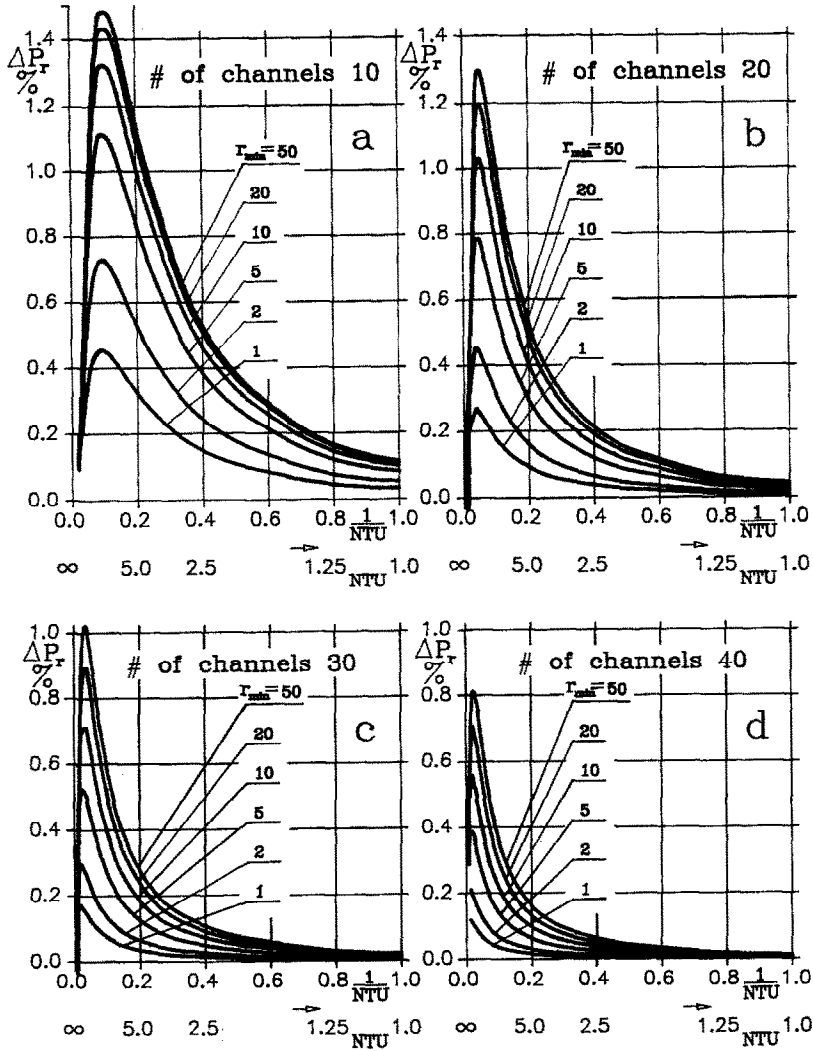


FIG. 5. Deviations of effectiveness $\Delta P_r = P_{r_{min}} - P_{r_{min}=0}$ (%) for different r_{min} from the effectiveness for $r_{min} = 0$ vs $1/NTU$ for ratio $R = 1$ and different numbers of channels n . (a) $n = 10$ (five turns); (b) $n = 20$; (c) $n = 30$; (d) $n = 40$.

changer, in this paper the manner presented in ref. [2] (diagrams: P_I, P_{II}) was chosen.

Since the biggest deviations in thermal effectiveness occur for a small number of channels, diagrams P_I vs P_{II} were drawn for number of turns $n = 4, 6, 8, 10, 12, 16, 20, 24, 30$ and 40 . As a minimal radius r_{min} values $2, 3, 4$ and 5 were selected for $n = 4, 6, 8$ and 10 , respectively. For values $n > 10$ the computations were carried out for constant value $r_{min} = 5$.

To see how good the counterflow SHE is in comparison to the true counterflow heat exchanger (acronym TCHE) in Fig. 6 the line with constant values of correction factor F was drawn ($F = 0.99, 0.97, 0.95, 0.93, 0.9, 0.8, 0.7$ and 0.6). The greater the areas outlined by axes P_I, P_{II} and curve with constant $F = 0.99, 0.97, 0.95, \dots$ the closer is the effectiveness of SHE to the ideal case of TCHE.

Another bunch of curves marked on the diagrams P_I vs P_{II} symbolizes the constant quantities of

$NTU = 0.1, 0.2, 0.3, 0.4, 0.5, 0.6, 0.8, 1.0, 1.2, 1.4, 1.6, 1.8, 2.0, 2.5, 3.0, 3.5, 4.0, 5, 6, 8, 10$ and 15 , which for $R < 1$ represent values NTU_I and for $R > 1$ values NTU_{II} .

6. CONCLUSIONS

Thermal features of SHE are evaluated with reference to the ideal case, i.e. TCHE with the help of the correction factor F . The lines with constant quantities of F marked on the diagrams P_I vs P_{II} represent the deviations of effectiveness of SHE from TCHE. Comparison should also be done regarding NTU and the number of channels n in SHE.

Consider the diagrams in Fig. 6: for those quantities of $NTU < 1$ any kind of heat exchanger does not differ remarkably from TCHE and therefore there is no necessity to emphasize the advantages of SHE. However, beginning from $NTU = 1$ and passing

(a)

Counterflow Spiral Heat Exchanger

channel's # = 2 * turn's #

4 = 2 * 2

$r_{min} = 2 b$

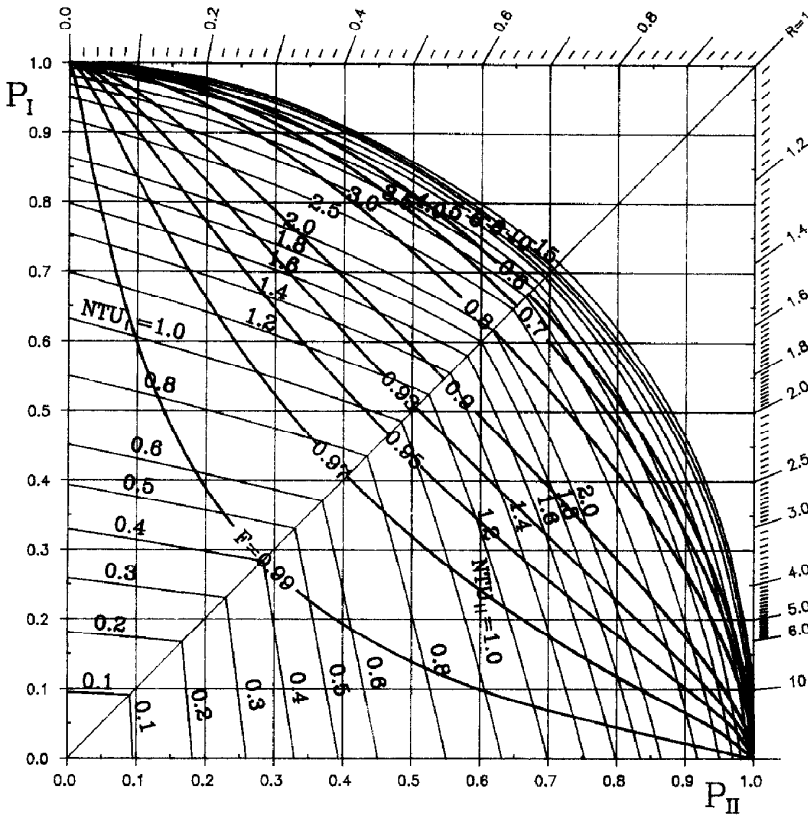
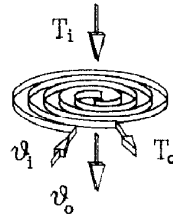


FIG. 6. Effectiveness of countercurrent spiral heat exchangers for different number of channels. (a) $n = 4$; (b) $n = 6$; (c) $n = 8$; (d) $n = 10$; (e) $n = 12$; (f) $n = 16$; (g) $n = 20$; (h) $n = 24$; (i) $n = 30$; (j) $n = 40$.

through the practical interval of $NTU = 2, 3$ even up to 4, one can see that the lines with $F = 0.99, 0.97$ or 0.95 (deviations of mean temperature distribution between SHE and TCHE of 1, 3 or 5%) include just this practical area of NTU .

It can be stated that starting from the number of channels $n = 20$ (10 turns) and more, for the most common interval of $NTU < 3$, the deviations of both effectivenesses are smaller than 3%. Generally speaking the higher the number of channels in SHE the closer are the effectivenesses of SHE and TCHE. On the basis of ref. [2], where different arrangements of flow are revised and diagrams P_I, P_{II} with the lines for $F = \text{constant}$ are plotted, one can testify that in the practical interval of NTU , SHE has higher effectivenesses than (almost) any other arrangement of flow, except TCHE.

For very high quantities of NTU of 10 to 30 or 40, dependent on the number of turns, the effectiveness

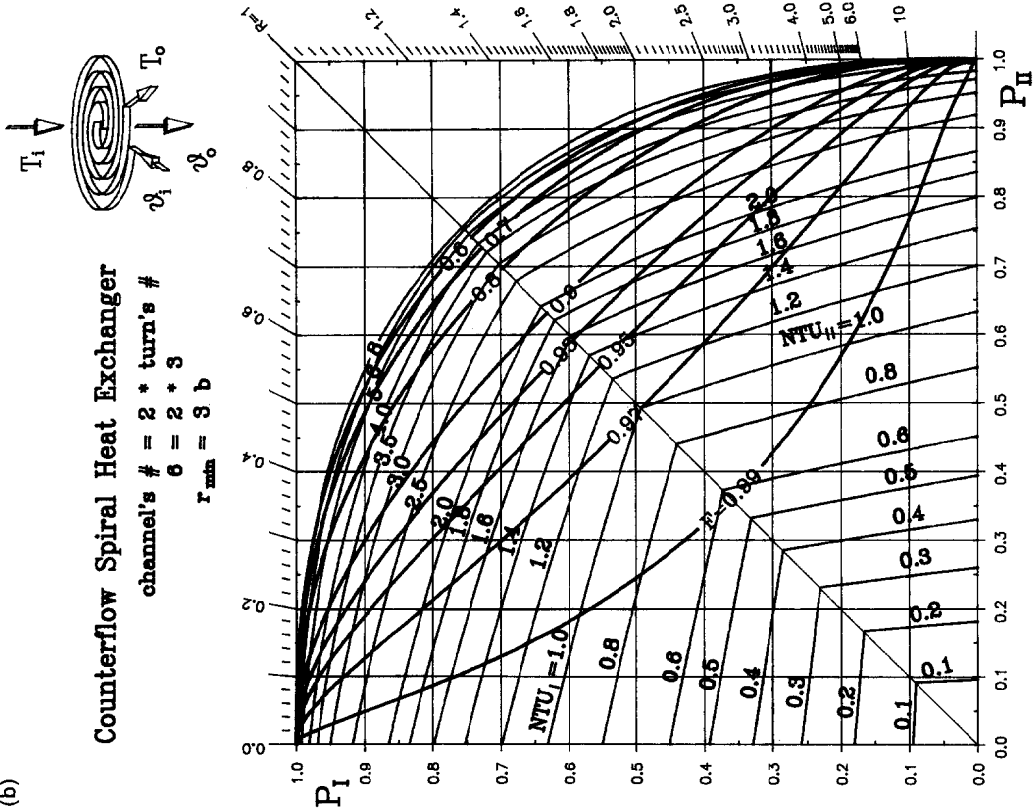
of SHE achieves its maximum and then with further growth of NTU decreases.† Particularly, if the ratio $R = 1$ then referring to number of channels $n = 6, 8, 10, 12, 14, 16, 18, 20, \dots, 30, \dots$ the effectiveness achieves its maximum for $NTU = 7.66, 9.34, 11.36, 13.25, 15.61, 17.50, 19.27, 21.63, \dots, 31.85, \dots$, respectively. In this interval of NTU the SHE loses its superiority over other arrangements of flow.

The influence of minimal radii on the effectiveness is small and for the number $n > 20$ the absolute deviation in the effectiveness does not exceed 0.2% or $\pm 0.1\%$, if comparison was referred to the effectiveness calculated for $r_{min} \leq 5$.

The Q-version of theoretical treatment is true no matter what arrangement of fluid flow in SHE is considered: counter- or cocurrent. The system of equa-

† This does not refer to $n = 4$ channels.

(b)



(c)

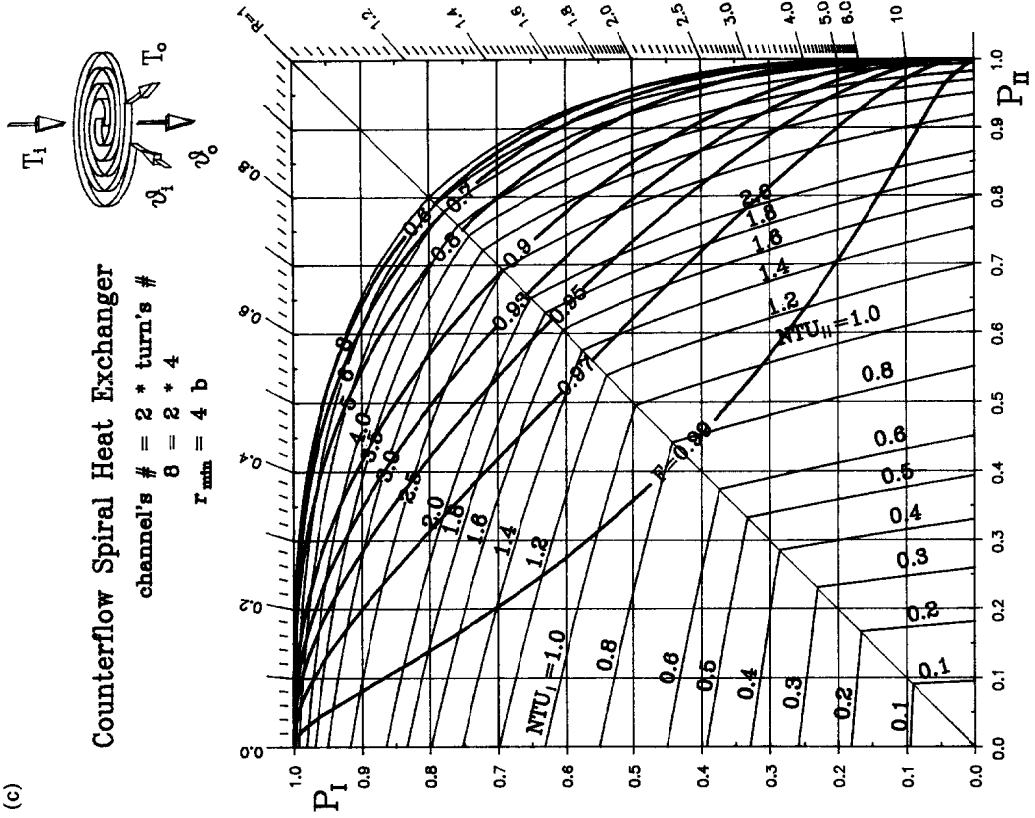
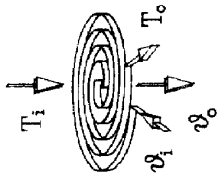


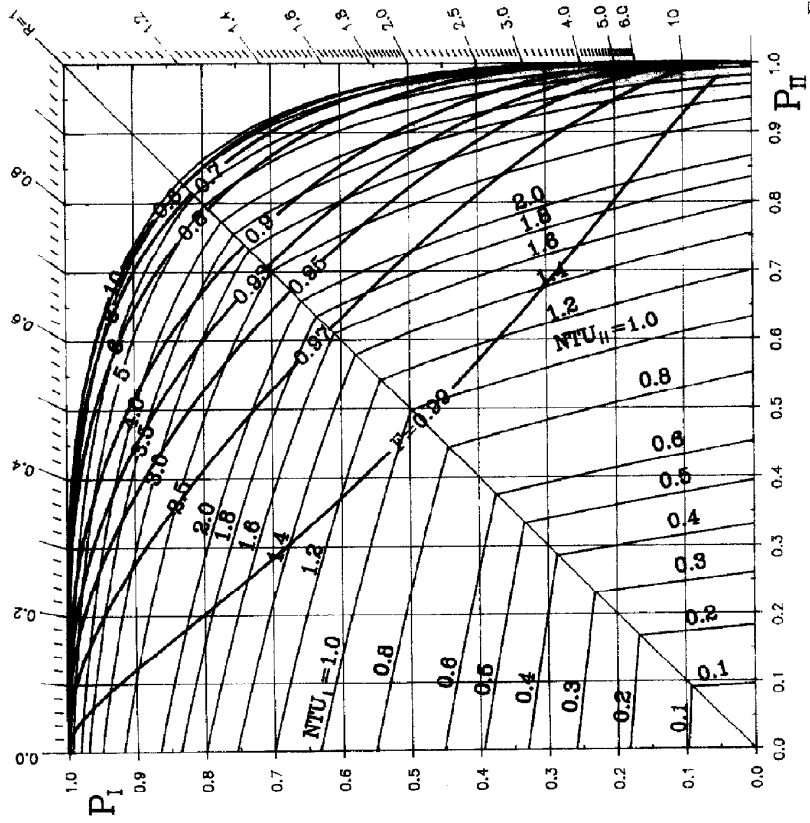
FIG. 6—Continued.

(d)

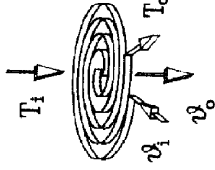


Counterflow Spiral Heat Exchanger

channel's # = 2 * turn's #
 10 = 2 * 5
 $r_{min} = 5 b$



(e)



Counterflow Spiral Heat Exchanger

channel's # = 2 * turn's #
 12 = 2 * 6
 $r_{min} = 5 b$

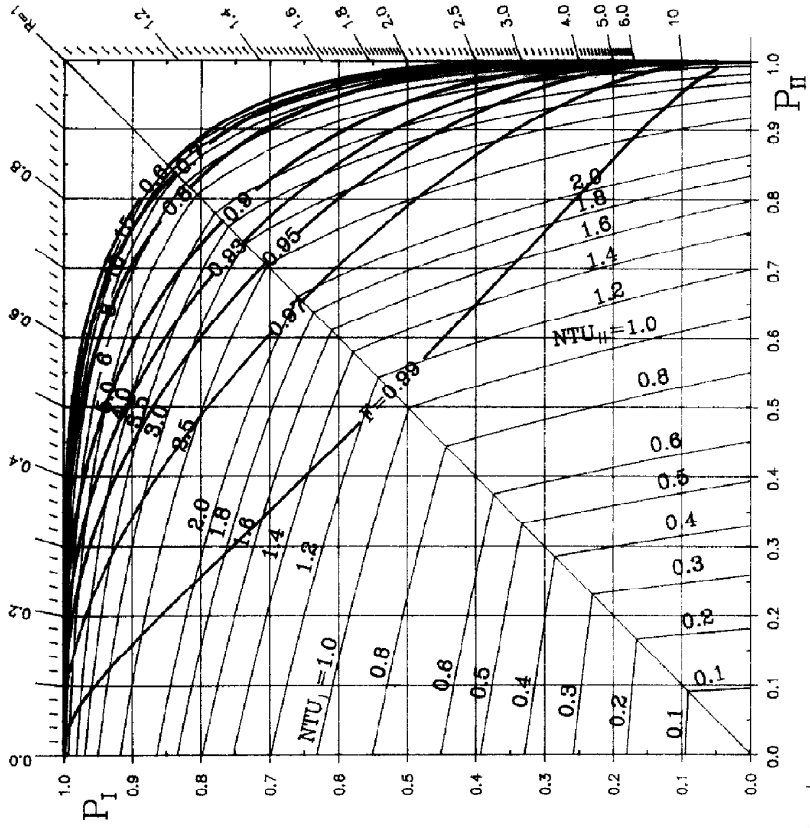


FIG. 6—Continued.

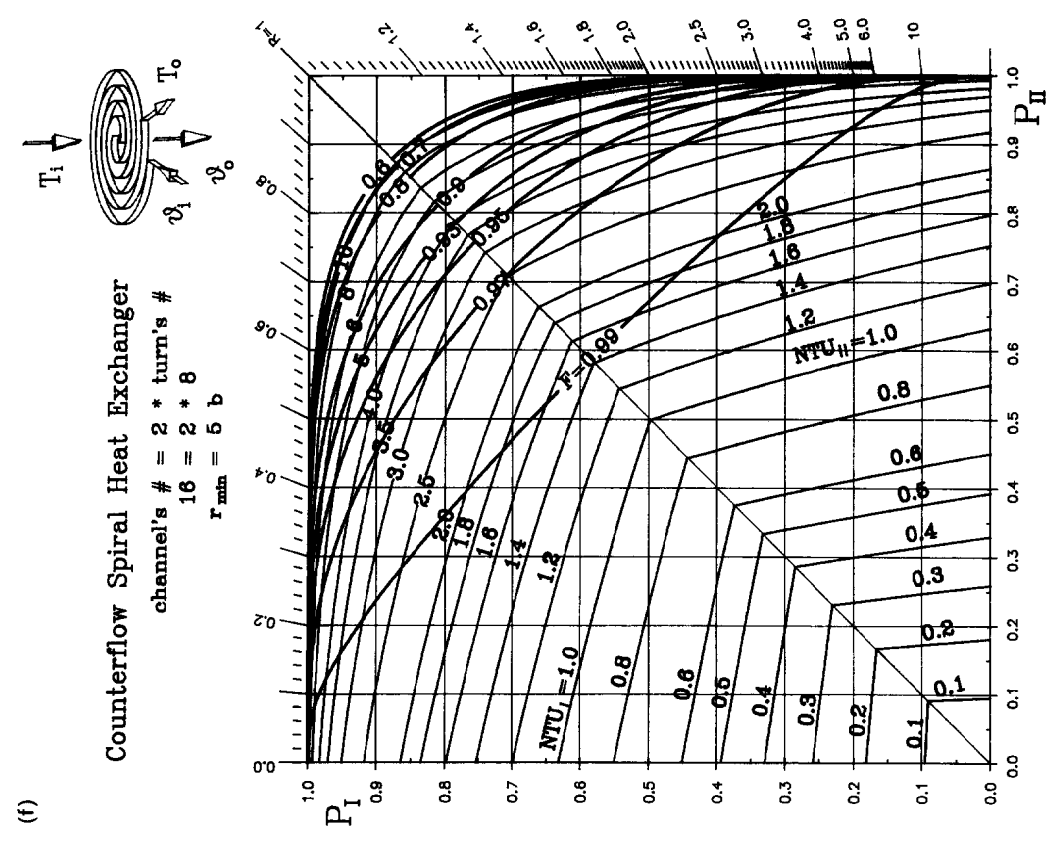
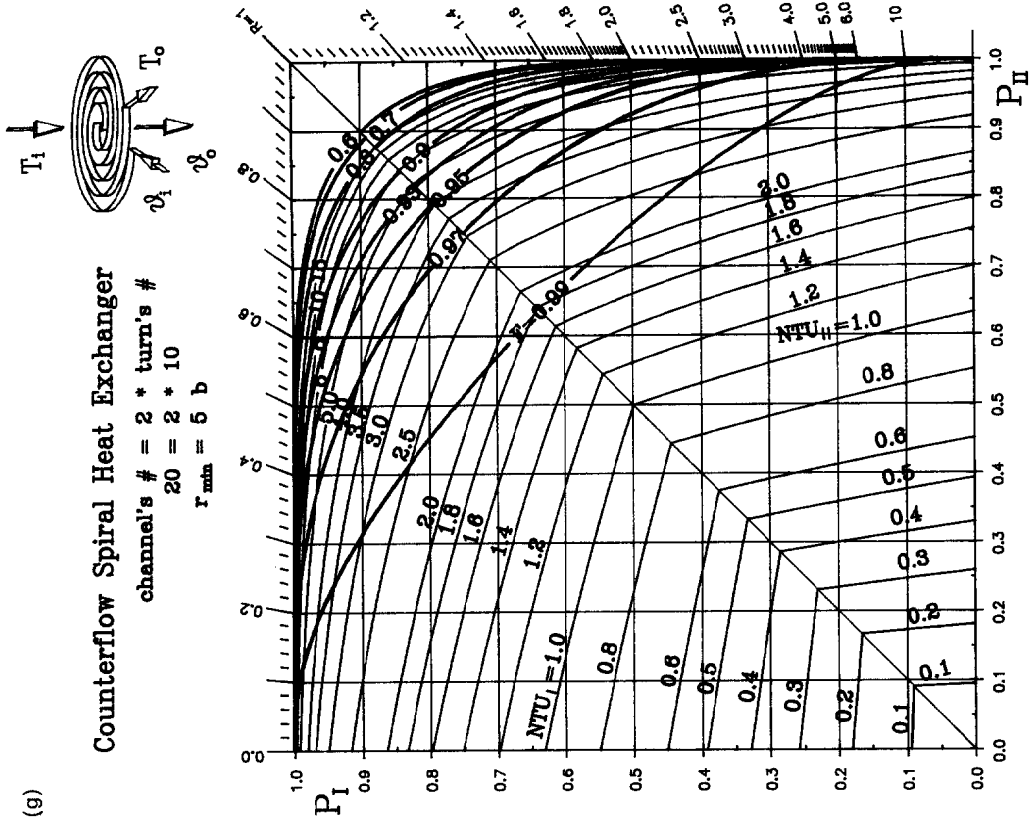


FIG. 6—Continued.

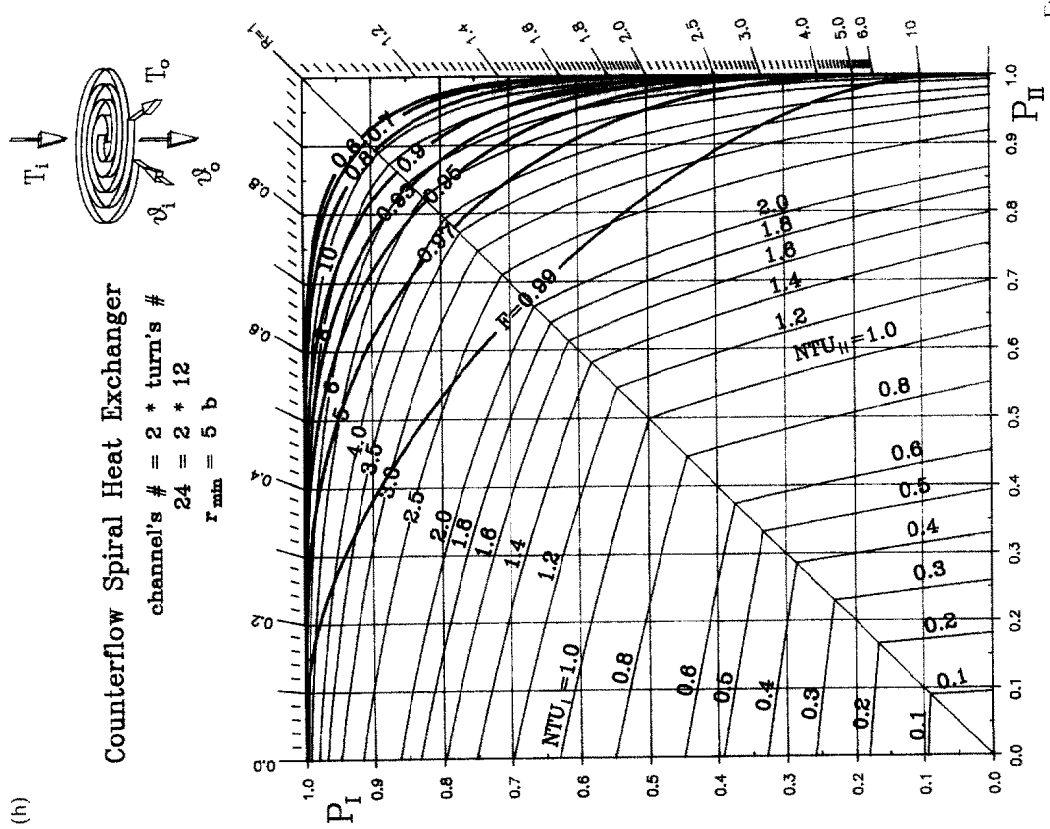
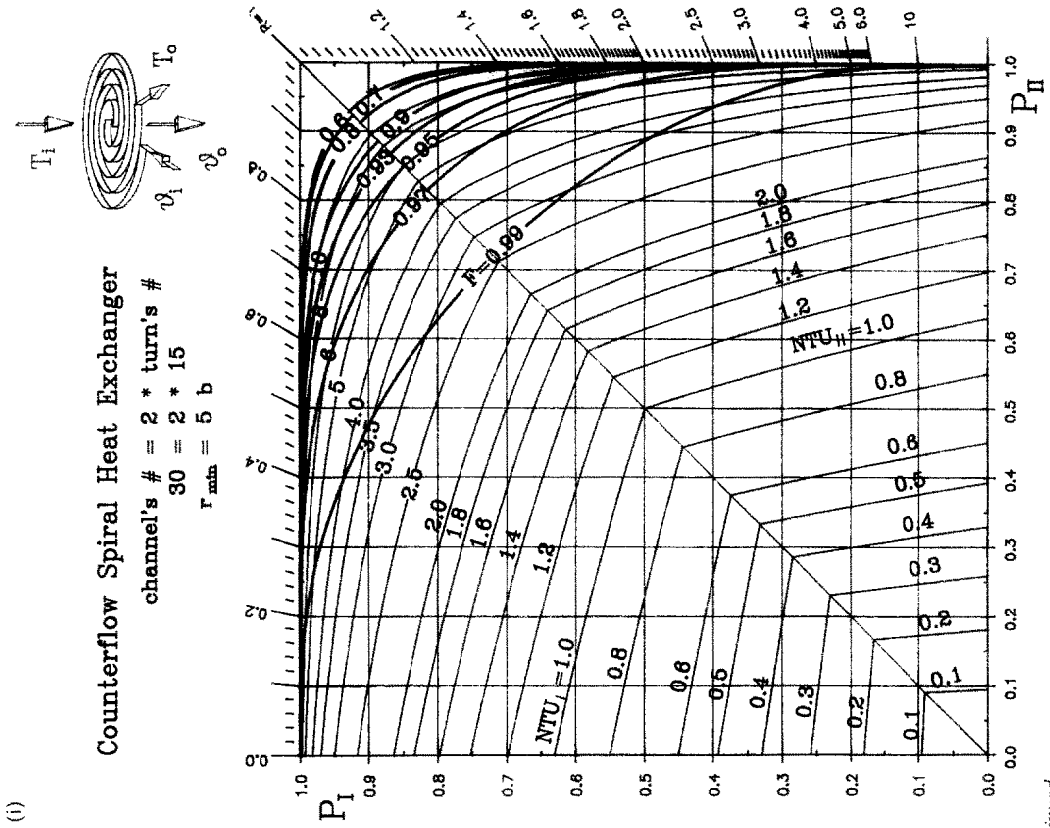


FIG. 6—Continued.

(i)

Counterflow Spiral Heat Exchanger

$$\text{channel's \#} = 2 * \text{turn's \#}$$

$$40 = 2 * 20$$

$$r_{\text{min}} = 5 b$$

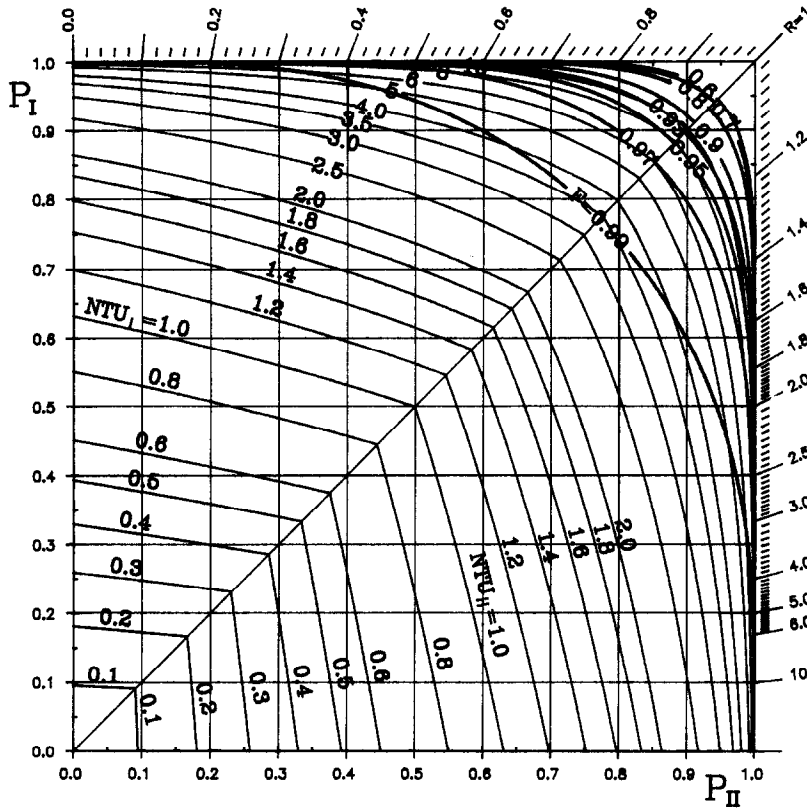
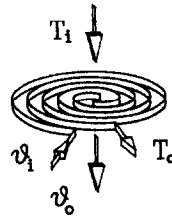


FIG. 6.—Continued.

tions (6) with appropriate conditions (9)–(11) is valid for cocurrent flow with ratio $R < 0$ (put into equation (8)), but only relation (12) has to be rewritten appropriately to this flow arrangement.

Acknowledgements—This research was carried out as a project for the Deutsche Forschungsgemeinschaft (DFG). The authors are greatly indebted to DFG for enabling and generously supporting this work.

REFERENCES

1. E. S. Gaddis, D. B. Spalding and J. Taborek, Heat exchanger theory, *Heat Exchanger Design Handbook*, Vol. I. VDI-Verlag GmbH, Hemisphere, Washington (1986).
2. W. Roetzel, Berechnung von Wärmeübertragern, *VDI-Wärmeatlas*, Chapter C, 5th edn. VDI-Verlag, Dusseldorf (1988).
3. Th. Bes, Eine Methode der thermischen Berechnung von Gegen- und Gleichstrom-Spiralwärmeaustauschern, *Wärme- und Stoffübertragung* **21**, 301–309 (1987).
4. J. Madejski, *Teoria Wymiany Ciepła (Theory of Heat Exchange)*, pp. 381–386. PWN Warszawa, Poznan (1963).
5. R. A. Buonopane and R. A. Troupe, Analytical and experimental heat transfer studies in a spiral plate heat exchanger, *IVth Int. Heat Transfer Conf.*, Vol. 1, HE 2.5, Paris (1970).
6. T. Zaleski and W. Krajewski, Metoda Obliczania Wymienników Spiralnych (Method of calculation for spiral exchangers), *Inżynieria Chemiczna (Chem. Engng)* **II**, 35–51 (1972).
7. J. P. Cieslinski and T. Bes, Analytical heat transfer studies in spiral plate heat exchangers, Reprints of XVIth Congr. of Refrigeration, Institut International du Froid (I.I.F.), Paris, pp. 67–72 (1983).
8. E. Morimoto and K. Hotta, Study of the geometric structure and heat transfer of a spiral plate heat exchanger, *Heat Transfer—Jap. Res.* **17**, 53–71 (1988).
9. G. Woschni, Die Berechnung von Spiralwärmeaustauschern, *Z. Techn. Hochschule Dresden* **9**, Heft 1 (1959/60).
10. W. Nowak, Obliczenia Rekuperatorów z Uwzględnieniem Strat do Otoczenia (Calculation of heat exchangers considering heat losses to the environment), *Zeszyty Naukowe Pol. Szczecińskiej (Scientific Journals Tech. Univ. of Stettin)* No. 114 (1969).
11. H. Martin, K. Chowdhury, H. Linkmeyer and K. M. Bassiouny, Straightforward design formulae for

efficiency and mean temperature difference in spiral plate heat exchanger. *VIIIth Int. Heat Transfer Conf.*, Vol. 6, pp. 2793–2797, San Francisco (1986).

12. N. Zhang, Z. Jiao and Z. Ni, A computational method for thermal design of spiral plate heat exchanger, *ASME Proc. National Heat Transfer Conf.*, HTD-96, Vol. 1, pp. 445–449 (1988).
13. V. N. Faddeeva, *Computational Methods of Linear Algebra*. Dover, New York (1959).
14. G. A. Korn and T. M. Korn, *Mathematical Handbook for Scientists and Engineers*, Vol. 1, Chapters 8, 13. McGraw-Hill, New York (1968).

APPENDIX: MATHEMATICAL TREATMENT OF THE DIFFERENTIAL EQUATIONS REPRESENTING THE ENERGY BALANCE

Method of solution

A common technique in the theory of linear differential equations is the method of Laplace's integrals. In this approach one considers a set of homogeneous linear differential equations with constant coefficients and constructs, directly, an integral representation of the solution. All of these requirements are fulfilled in equation (6) and appropriate boundary conditions (9)–(12).

Let us denote Laplace's parameter by s and the transformed vector q by $f(s) = \mathcal{L}[q(\omega)]$. Utilizing transformation \mathcal{L} equations (6) become

$$[sI + M]f(s) = q(0) \tag{A1}$$

where I is the unit matrix of the same order as M . The equation

$$[sI + M] = 0 \tag{A2}$$

is called the characteristic equation of M and determines those values s (eigenvalues) which are the basis for the construction of a general solution.

When calculating the effectiveness and/or temperatures of fluids using the method proposed here, the most time consuming calculations are those of the matrix $[sI + M]$ (equations (7) and (A2)) and even more the numerators N_{ij} in equation (14). This is because each subscript i and j in numerator N runs from 1 to $n-1$, which makes it necessary to compute it $(n-1)^2$ times. All these operations have to be repeated $n-1$ times for each eigenvalue s_i ; together this gives $(n-1)^3$ determinants.

Calculation of determinant $[sI + M]$. There is a proposal to select submatrices from matrix $[sI + M]$ by way of cutting out the square submatrix (subdeterminant) from its right bottom corner. This subdeterminant, which has rank $(n-1-j)$, is denoted by $D_j(s)$. It can easily be proved that there exists a connection between the three subdeterminants $D_{j-1}(s)$, $D_j(s)$ and $D_{j+1}(s)$:

$$D_{j-1}(s) = (s + r_{j-1}d)D_j(s) - c_{j-1}^2 r_j r_{j-1} D_{j+1}(s) \tag{A3}$$

where quantities d and c_j are explained in equation (8). Starting from two of the initial values $D_{n+1}(s) = 0$, $D_n(s) = 1$ and running backwards with subscripts j from n to 2, one arrives at $D_1(s)$, which is equal to the sought determinant value of the matrix $[sI + M]$. The set of data D_j for $j = 1, 2, \dots, n-2, n-1$ should be stored. This same procedure is valid for the derivative of the subdeterminant with regard to parameter s , $dD_j(s)/ds$, which appears in equation (14).

The application of the recurrent form (equation (A3)) allows one to save a number of multiplications and divisions necessary to the computation of a determinant of order $n-1$ from $(n-2)(n^2-n+3)/3$ in a standard case (see p. 73 of ref. [14]) to $\sim 2(n-1)$ in the present proposal.

Calculation of numerators N_{ij} . The numerator $N(s_j)$ with subscripts i and j , made from matrix $[sI + M]$ according to the prescription explained in Section 3.4, has the following form:

		column i					
	$N_{ij} =$	$s + r_1 d$	$-c_1 \sqrt{(r_1 r_2)}$	0	\vdots	0	
		$-c_1 \sqrt{(r_1 r_2)}$	$s + r_2 d$	0	\vdots	0	
		0	$c_2 \sqrt{(r_2 r_3)}$	0	$-c_3 \sqrt{(r_3 r_4)}$	\vdots	0
row j		0	0	1	0	\vdots	0
		0	0	0	\vdots	0	
		0	0	0	\vdots	0	
				$s + r_{n-2} d$	$c_{n-2} \sqrt{(r_{n-2} r_{n-1})}$	0	
				$c_{n-2} \sqrt{(r_{n-2} r_{n-1})}$	$s + r_{n-1} d$	0	

Since further steps towards the solution are more of a mathematical exercise these considerations are abandoned and only the results unique for the present task will be presented. More information about this standard solution can be found in the proper mathematical literature, e.g. ref. [14].

General instructions for numerical calculations

For the problem under consideration it is possible to propose some improvements in the method of calculation, focusing on the compact recurrent formula which allows one to avoid frequent laborious computation of matrices.

A decision about a tool which can be used to compute the effectiveness accurately is up to the designer. However, in the authors' opinion, he should have the possibility of achieving this goal on a personal computer. Therefore advice on the straightforward way of numerical operations is necessary and it has to be outlined here.

Let us store the set of data computed as a product of coefficients which lie on a subdiagonal of matrix M . For $j = 0$, $p_0 = 1$ and $j = 1, 2, 3, \dots, n-2$

$$p_i = \prod_{k=1}^{i=j} c_k \sqrt{(r_k r_{k+1})} \tag{A5}$$

where $c_k \sqrt{(r_k r_{k+1})}$ are components of the matrix equation (7).

The value of numerator $N_{ij}(s_i)$ can be calculated as follows: consider $i < j$ and replace the symbols D_{j-1} , D_j , D_{j+1} in equation (A3) by B_{j-1} , B_j , B_{j+1} , respectively. In this case the form of equation (A3) is still valid under the condition that the recurrent operation starts from subscript i running backwards to 2 and that now the other initial values of B_i , B_{i+1} should be used. Omitted from the analysis here are the two initial values calculated as follows: $B_{i+1} = 0$ and $B_i = D_{i+1} p_{i-1} / p_{i-1}$, where D_{j+1} was determined and stored before. The value of $-(-1)^j B_i(s_i)$ computed according to the described procedure is equal to the sought numerator $N_{ij}(s_i)$. Using the advantage of the symmetry of matrix M it

can be stated that $N_{ij}(s_i) = N_{ji}(s_j)$. For subscripts $j = i$ this procedure is in force as well.

It should be mentioned that by computation of all values N_{ij} in accordance to described procedure the number of operations is additionally reduced for two reasons. First,

almost twice because of its symmetry (exact proportion is $[1 + 1/(n-1)]/2$) and second because of the different position of the subscripts i and j in the triangular matrix the initial value B_i starts from $i < n-1$, which allows for a decrease in these operations by approximately one third as well.

DISTRIBUTION DE LA DENSITE DE FLUX THERMIQUE DANS LES ECHANGEURS SPIRALES

Résumé—On développe une méthode analytique pour le calcul précis des changements de température dans les échangeurs thermiques spirales à contre-courant. La spirale est composée de profils en arc de cercle avec centres de courbure aux sommets d'un triangle équilatéral. On suppose constants les coefficients de transfert et les capacités thermiques. Contrairement à la procédure conventionnelle, on s'intéresse à la distribution de densité de flux thermique, ce qui offre des avantages considérables par rapport à l'analyse directe des températures du fluide. On étudie l'influence des différents paramètres géométriques et des graphes sont présentés pour le dessin et l'évaluation des échangeurs thermiques spirales.

VERTEILUNG DER WÄRMESTROMDICHTEN IN SPIRAL-WÄRMEÜBERTRAGERN

Zusammenfassung—Es wird eine analytische Methode entwickelt zur genauen Berechnung der Temperaturänderung in Gegenstromspiralwärmeübertragern. Die Spirale ist aus Kreisbögen zusammengesetzt mit den Krümmungsmittelpunkten auf den Eckpunkten eines gleichseitigen Dreiecks. Es werden konstante Wärmedurchgangskoeffizienten und Wärmekapazitäten vorausgesetzt. Im Gegensatz zur üblichen Behandlungsweise wird die Verteilung der Wärmeflußdichte betrachtet, was beachtliche Vorteile gegenüber einer direkten Untersuchung der Fluidtemperaturen bringt. Der Einfluß verschiedener geometrischer Daten wird untersucht, und es werden Diagramme für den Entwurf und das Nachrechnen von Spiralwärmeübertragern vorgelegt.

РАСПРЕДЕЛЕНИЕ ПЛОТНОСТИ ТЕПЛООВОГО ПОТОКА В СПИРАЛЬНЫХ ТЕПЛООБМЕННИКАХ

Аннотация—Разработан аналитический метод точного расчета изменения температуры в противоточных спиральных теплообменниках. Змеевик имеет кольцевой профиль с центрами кривизны на углах равностороннего треугольника. Предполагается постоянство суммарного коэффициента теплопереноса и теплоемкости. В противоположность общепринятой методике рассматривается распределение плотности теплового потока, что дает значительные преимущества по сравнению с прямым анализом температур жидкости. Исследуется влияние различных геометрических параметров, и представлены графики для проектирования и оценки спиральных теплообменников.